# The hybrid radio/X-ray correlation of the black hole transient MAXI J1348–630

F. Carotenuto, S. Corbel, E. Tremou, T.D. Russell, A. Tzioumis, R.P. Fender, P.A. Woudt, S.E. Motta, J.C.A. Miller-Jones, A.J. Tetarenko, et al.

Monthly Notices of the ROYAL ASTRONOMICAL SOCIETY

MNRAS **505,** L58–L63 (2021) https://doi.org/10.1093/mnrasl/slab049
Advance Access publication 2021 May 21

# The hybrid radio/X-ray correlation of the black hole transient MAXI J1348–630

F. Carotenuto [1]★ S. Corbel,[1,2] E. Tremou [3] T. D. Russell [4] A. Tzioumis,[5] R. P. Fender,[6,7] P. A. Woudt [7] S. E. Motta [6] J. C. A. Miller-Jones [8] A. J. Tetarenko [9] and G. R. Sivakoff[10]

[1]*AIM, CEA, CNRS, Université de Paris, Université Paris-Saclay, F-91191 Gif-sur-Yvette, France*
[2]*Station de Radioastronomie de Nançay, Observatoire de Paris, CNRS, PSL Research University, Univ. Orléans, F-18330 Nançay, France*
[3]*LESIA, Observatoire de Paris, CNRS, PSL Research University, Sorbonne Université, Université de Paris, Meudon F-92195, France*
[4]*INAF, Istituto di Astrofisica Spaziale e Fisica Cosmica, Via U. La Malfa 153, I-90146 Palermo, Italy*
[5]*Australia Telescope National Facility, CSIRO, PO Box 76, Epping, NSW 1710, Australia*
[6]*Astrophysics, Department of Physics, University of Oxford, Keble Road, Oxford OX1 3RH, UK*
[7]*Department of Astronomy, Inter-University Institute for Data-Intensive Astronomy, University of Cape Town, Private Bag X3, Rondebosch 7701, South Africa*
[8]*International Centre for Radio Astronomy Research, Curtin University, GPO Box U1987, Perth, WA 6845, Australia*
[9]*East Asian Observatory, 660 N. A'ohōkū Place, University Park, Hilo, HI 96720, USA*
[10]*Department of Physics, University of Alberta, CCIS 4-181, Edmonton, AB T6G 2E1, Canada*

Accepted 2021 May 10. Received 2021 May 10; in original form 2021 April 1

## ABSTRACT

Black hole (BH) low mass X-ray binaries in their hard spectral state are found to display two different correlations between the radio emission from the compact jets and the X-ray emission from the inner accretion flow. Here, we present a large data set of quasi-simultaneous radio and X-ray observations of the recently discovered accreting BH MAXI J1348–630 during its 2019/2020 outburst. Our results span almost six orders of magnitude in X-ray luminosity, allowing us to probe the accretion–ejection coupling from the brightest to the faintest phases of the outburst. We find that MAXI J1348–630 belongs to the growing population of outliers at the highest observed luminosities. Interestingly, MAXI J1348–630 deviates from the outlier track at $L_X \lesssim 7 \times 10^{35}(D/2.2\ \mathrm{kpc})^2$ erg s$^{-1}$ and ultimately rejoins the standard track at $L_X \simeq 10^{33}(D/2.2\ \mathrm{kpc})^2$ erg s$^{-1}$, displaying a hybrid radio/X-ray correlation, observed only in a handful of sources. However, for MAXI J1348–630 these transitions happen at luminosities much lower than what observed for similar sources (at least an order of magnitude). We discuss the behaviour of MAXI J1348–630 in light of the currently proposed scenarios and highlight the importance of future deep monitorings of hybrid correlation sources, especially close to the transitions and in the low luminosity regime.

**Key words:** accretion, accretion discs – black holes physics – stars: individual: MAXI J1348–630 – ISM: jets and outflows – radio continuum: stars – X-rays: binaries.

## 1 INTRODUCTION

Black holes (BH) low mass X-ray binaries (LMXBs) are binary systems comprising a BH that accretes matter from a low mass companion star. Occasionally, these systems enter outburst phases during which the X-ray luminosity is greatly variable and several transitions between distinct accretion states are observed (e.g. Remillard & McClintock 2006; Belloni & Motta 2016; Corral-Santana et al. 2016; Tetarenko et al. 2016). A strong coupling exists between accretion and ejection in BH LMXBs, as the relativistic jets powered by these sources are highly dependent on the state of the accretion disc. From an observational point of view, BH LMXBs in the hard spectral state are characterized by a non-linear correlation between the radio and X-ray luminosities ($L_R \propto L_X^{\beta}$, e.g. Hannikainen et al. 1998; Corbel et al. 2000; Gallo, Fender & Pooley 2003). Based on scale-invariant properties of BH accretion and jet production, this correlation has also been extended to active galactic nuclei by including the mass as an additional parameter (Merloni, Heinz & di Matteo 2003; Falcke, Körding & Markoff 2004; Plotkin et al. 2012). BH LMXBs are divided in two populations which lie on two different tracks of the radio/X-ray diagram. Originally, the few 'historical' BH sources were found to lie on a track labelled as standard, with a power-law index $\beta \sim 0.6$ (such as GX 339–4, V404 Cyg, and now also MAXI J1820+070, Corbel et al. 2000, 2003, 2013; Gallo et al. 2003; Bright et al. 2020; Shaw et al. 2021). These sources appear to maintain this correlation down to the quiescent level (Corbel et al. 2013; Gallo et al. 2019; Tremou et al. 2020). As new observations accumulate, more and more sources (labelled outliers) were found to lie on a different branch, well below the standard track, with a steeper slope $\beta \gtrsim 1$ (Coriat et al. 2011). We note that in some works the two populations are referred to as radio-loud and radio-quiet, one of the two ways to interpret the data, see Coriat et al. (2011) for more details. Outliers could be characterized by more negative radio spectral indices (Espinasse & Fender 2018) and lower rms variability (Dinçer et al. 2014; Motta, Casella & Fender 2018) with respect to

★ E-mail: francesco.carotenuto@cea.fr

standard track sources, which may be indications for understanding the nature of the two different tracks. While the reasons for the the existence of this dichotomy are still unclear, several explanations for the observed scenario have been proposed. A physical difference in the disc–jet coupling may be responsible for the two groups. This could originate from the structure of the inner accretion flow or alternatively the properties of jets might differ between the two tracks, causing different levels of radio emission (Coriat et al. 2011; see also Section 4 for more details). The existence of the two tracks has also been questioned statistically (e.g. Gallo et al. 2014; Gallo, Degenaar & van den Eijnden 2018) if one considers the whole sample of sources. However, it is particularly important to precisely track the behaviour of specific sources, such as H1743–322 (Coriat et al. 2011; Williams et al. 2020), for which the path on the diagram is very clear, to pinpoint the overall behaviour which may be masked in the whole sample due to overlap of sources and possible transition between the two tracks.

In this letter, we present radio and X-ray observations of MAXI J1348–630 to highlight its behaviour on the radio/X-ray diagram. Thanks to the deep and long term coverage of our multi-wavelength monitoring, we are able to probe the source behaviour on the radio/X-ray diagram in great detail, from the bright phases, down to the lowest level of emission in outburst, when the source is close to its quiescent state. So far, this has been possible for only a limited number of sources, especially over a single outburst (see for instance Corbel et al. 2013; Shaw et al. 2021). MAXI J1348–630 is a new BH LMXB discovered in 2019 January (Yatabe et al. 2019; Tominaga et al. 2020), located at a distance $D = 2.2^{+0.6}_{-0.5}$ kpc (Chauhan et al. 2021). We note that Lamer et al. (2021) recently reported a distance $D = 3.39 \pm 0.34$ kpc from observations with eROSITA. While in this paper we assume $D = 2.2$ kpc, to include the second distance measurement we quote all derived luminosities with a factor $(D/2.2\ \mathrm{kpc})^2$. In Carotenuto et al. (2021) we have presented the full X-ray and radio monitoring of the source during its 2019/2020 outburst. The source first completed a whole cycle in the hardness-intensity diagram (HID) and then exhibited a sequence of hard state re-brightenings (e.g. Al Yazeedi et al. 2019; Russell et al. 2019b; Pirbhoy et al. 2020). Our radio observations detected and monitored the rise, quenching and re-activation of compact jets through the different phases of the outburst. In addition, single-sided and resolved discrete ejecta were detected (Carotenuto et al. 2021). Two jet components were launched ∼2 months apart and both displayed a very high proper motion ($\gtrsim 100$ mas d$^{-1}$).

## 2 OBSERVATIONS

MAXI J1348–630 has been monitored with MeerKAT (Jonas & MeerKAT Team 2016; Camilo et al. 2018) at 1.28 GHz, as part of the ThunderKAT Large Survey Programme (Fender et al. 2018), and with the Australia Telescope Compact Array (ATCA) at 5.5 and 9 GHz. On the X-ray side, MAXI J1348–630 was regularly monitored by the Neil Gehrels *Swift* Observatory (Gehrels et al. 2004) with the X-ray Telescope (XRT; Burrows et al. 2005), and by the Monitor of All-sky X-ray Image (MAXI; Matsuoka et al. 2009). The full observing campaign on MAXI J1348–630 has already been presented in Carotenuto et al. (2021) and we refer to that work for details on the radio and X-ray data processing. In this work, we also include two additional detections of MAXI J1348–630 during its seventh hard state re-flare (2020 September–October, Carotenuto et al. 2020; Negoro et al. 2020), from observations performed with MeerKAT, ATCA, and *Swift*/XRT and not reported in Carotenuto et al. (2021).

## 3 THE RADIO/X-RAY CORRELATION OF MAXI J1348–630

To characterize the behaviour of MAXI J1348–630 in the radio/X-ray diagram, we selected epochs with quasi-simultaneous ($\Delta t \leq$ 24 h) radio and X-ray observations between MJD 58509 and 58522, and after MJD 58597, during which the system was in the hard and intermediate state (see Zhang et al. 2020 and Carotenuto et al. 2021 for details on the state transitions). For each epoch we converted the measured radio flux density $S_\nu$ to the 5 GHz monochromatic luminosity $L_\mathrm{R} = 4\pi D^2 \nu S_\nu$, assuming a distance $D = 2.2$ kpc and using either the measured spectral index $\alpha$ (see Table 1) when available, or the average spectral index $\langle\alpha\rangle = 0.14 \pm 0.01$. The unabsorbed 1–10 keV X-ray flux $S_\mathrm{X}$ obtained from *Swift*/XRT was converted to the integrated luminosity $L_\mathrm{X} = 4\pi D^2 S_\mathrm{X}$. For simultaneity, we selected *Swift* epochs taken less than 24 h before or after the corresponding radio observations. When this was not possible, we interpolated the X-ray flux from a exponential fit to the smoothly evolving *Swift*/XRT light curve, adding a conservative 10 per cent error on the interpolated X-ray fluxes and checking the consistency with the simultaneous MAXI data. This leads to a sample of 44 measurements on the radio/X-ray diagram, with a total of 39 detections of MAXI J1348–630 in radio and X-rays.

A sample of the flux values is reported in Table 1, while the full data set is provided as online supplementary material, and the radio/X-ray measurements of MAXI J1348–630 are shown in Fig. 1. We note that our monitoring allowed us to probe the behaviour of MAXI J1348–630 over six orders of magnitude in the X-ray luminosity and almost four in its radio luminosity, which so far has rarely been possible for XRBs. Moreover, our measurements include three detections at $L_\mathrm{X} < 10^{33}(D/2.2\,\mathrm{kpc})^2$ erg s$^{-1}$, which are of key importance to probe the accretion/ejection connection at the lowest luminosities. To allow a direct comparison, measurements of GX 339–4 (Corbel et al. 2013; Tremou et al. 2020) and H1743–322 (Coriat et al. 2011) are also shown, as the two sources are representative of the standard and outlier branches, respectively. MAXI J1348–630 immediately appeared to be incompatible with the standard track, being significantly fainter in radio than GX 339–4 below $L_\mathrm{X} < 10^{38}(D/2.2\ \mathrm{kpc})^2$ erg s$^{-1}$. For $L_\mathrm{X}$ between $\sim 5 \times 10^{35}$ and $10^{38}(D/2.2\ \mathrm{kpc})^2$ erg s$^{-1}$ the source appeared to follow a steep correlation, globally consistent with the population of outliers. We note that the track followed during the decay of the main outburst was brighter in radio with respect to the rising phase, possibly similar to the rise and decay phases of the 2010/2011 outburst of GX 339–4 (Corbel et al. 2013). For $L_\mathrm{X} \lesssim 5 \times 10^{35}(D/2.2\ \mathrm{kpc})^2$ erg s$^{-1}$, MAXI J1348–630 transitioned to a flatter correlation. Unlike the main outburst, the rise and decay of the first reflare are consistent with the same track. On MJD 58614, 58621, and 58628 the radio core detected with MeerKAT was not completely separated due to the presence of discrete ejecta, hence we put a caveat on the radio fluxes obtained from source fitting in those three epochs (the two detections with the lowest radio emission during the decay of the main outburst and the faintest radio detection during the rise of the first reflare, see Fig. 1. As $L_\mathrm{X}$ decreases, the source ultimately re-joins the standard track at $L_\mathrm{X} \simeq 10^{33}(D/2.2\ \mathrm{kpc})^2$ erg s$^{-1}$ and is clearly detected down to $\sim 10^{32}(D/2.2\ \mathrm{kpc})^2$ erg s$^{-1}$, displaying a behaviour similar to H1743–322 (Coriat et al. 2011), but transitioning between the two tracks at vastly lower radio and X-ray luminosities.

We fit our radio and X-ray data of MAXI J1348–630 using `curve_fit` from the SCIPY package to obtain a tentative estimation of the correlation slopes. Visual inspection shows that, given the evolution of MAXI J1348–630 on the diagram, a single power law does

**Table 1.** Sample of the radio flux densities and unabsorbed X-ray fluxes selected for the radio/X-ray correlation presented in this work, along with the radio spectral index (when available) and the telescopes used for obtaining the data (see Carotenuto et al. 2021). Here, we only show the rising phase of the main outburst, while the full table is available online as supplementary material. The radio spectral index is only computed for ATCA multifrequency observations.

| MJD | Outburst phase | X-ray flux[a] 1–10 keV | Radio flux density (mJy) | Spectral index $\alpha$ | Telescopes |
|---|---|---|---|---|---|
| 58509.9 | Main outburst – rise | 38.1 ± 0.3 | 3.4 ± 0.1 | 0.02 ± 0.09 | ATCA/*Swift* |
| 58511.0 | – | 201 ± 20 | 6.2 ± 0.4 | 0.1 ± 0.2 | ATCA/*Swift*[b] |
| 58512.0 | – | 346 ± 35 | 13.70 ± 0.05 | | MeerKAT/*Swift*[b] |
| 58514.0 | – | 528 ± 53 | 21.9 ± 0.8 | 0.18 ± 0.02 | ATCA/*Swift*[b] |
| 58515.2 | – | 590 ± 59 | 28.6 ± 0.1 | | MeerKAT/*Swift*[b] |
| 58515.9 | – | 625 ± 3 | 34.4 ± 1.4 | | ATCA/*Swift* |
| 58519.9 | – | 1320 ± 132 | 135 ± 1 | 0.155 ± 0.003 | ATCA/*Swift*[b] |

*Notes.* [a]In units of $10^{-10}$ erg cm$^{-2}$ s$^{-1}$. [b]Interpolated X-ray flux.

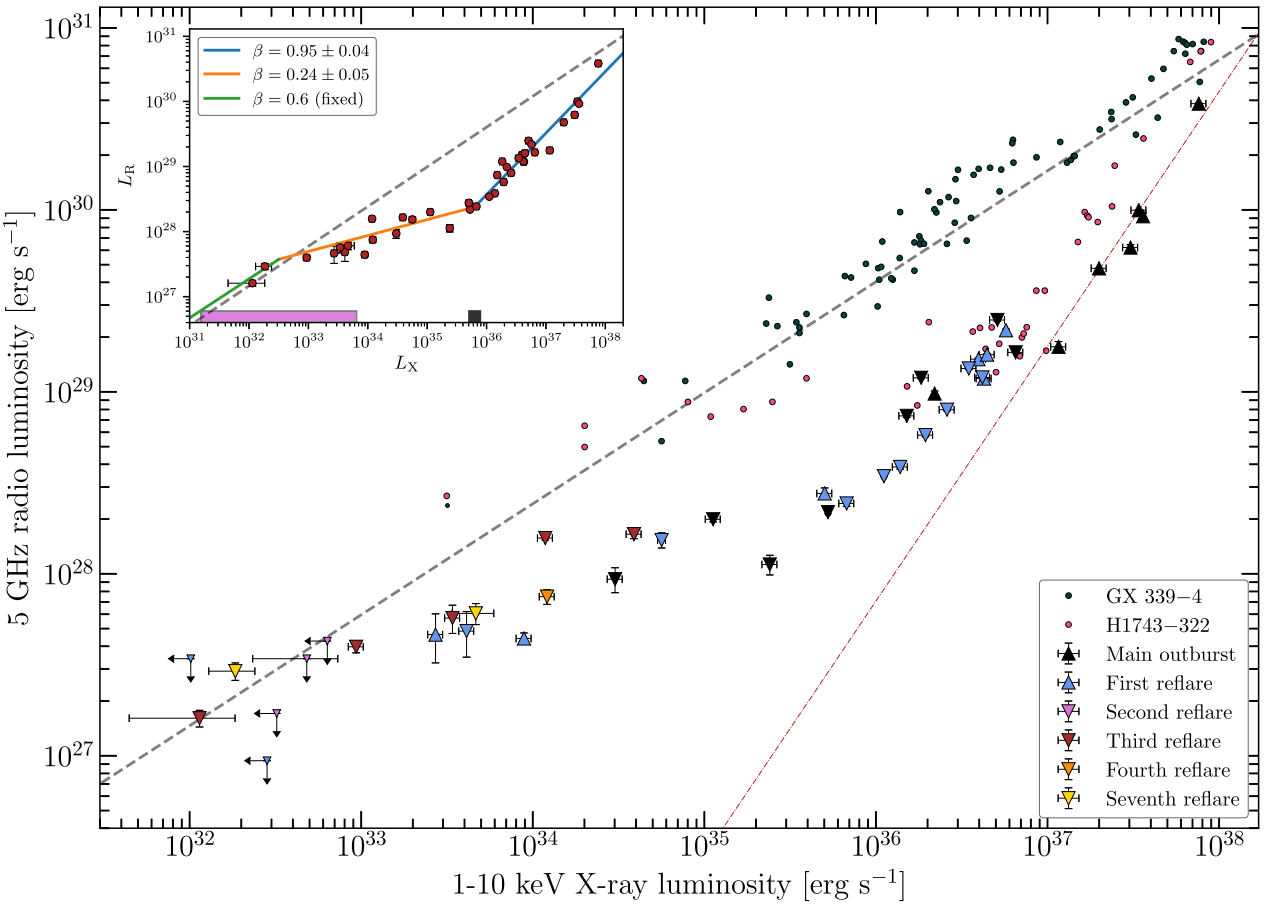


**Figure 1.** MAXI J1348–630 radio/X-ray diagram during its 2019/2020 outburst. We assume $D = 2.2$ kpc (Chauhan et al. 2021). Points from different phases of the outburst are plotted with different colours and triangles pointing upwards or downwards differentiate between, respectively, rise and decay. The red and grey dashed lines represent, respectively, the $\beta = 1.4$ and $\beta = 0.6$ correlations (see Section 1), and are shown for illustrative purposes. The source transitions between tracks while going from higher to lower luminosities. For comparison, H1743–322 (Coriat et al. 2011) and GX 339–4 (Corbel et al. 2013; Tremou et al. 2020) are shown on the diagram with smaller size points. A tentative fit to the same data is shown in the inset in the top-left corner. The magenta and grey rectangles represent the lower and upper bounds on the $x$-axis of, respectively, the $L_{\rm stand}$ and $L_{\rm trans}$ confidence intervals (see Section 3).

not appear to be adequate to fit the whole data set. Therefore, we adopt a double-broken power law, making the distinction between a steep branch followed when $L_{\rm X} \geq L_{\rm trans}$, a flatter correlation for $L_{\rm stand} < L_{\rm X} < L_{\rm trans}$, and assuming that the source follows the standard track with $\beta = 0.6$ for $L_{\rm X} \leq L_{\rm stand}$. We note that this fit is for illustrative purposes, and the results should only be taken as indicative, given the significant dispersion of the data obtained by merging the various phases of the outburst. The results of the fit are shown in the inset of Fig. 1. For the high luminosity part, we obtain a slope $\beta_{\rm steep} = 0.95 \pm 0.04$ with $L_{\rm trans} = 6.3^{+1.5}_{-1.2} \times 10^{35} (D/2.2\ {\rm kpc})^2$ erg s$^{-1}$, while the fit yields $\beta_{\rm flat} = 0.24 \pm 0.05$ for the flat branch. Since we fixed $\beta_{\rm stand} = 0.6$, the only parameter left is $L_{\rm stand}$, namely the transition luminosity between the flat branch and the standard track, which is not constrained by the fit, as we obtain: $L_{\rm stand} = 3.2^{+61.3}_{-3.0} \times 10^{32} (D/2.2\ {\rm kpc})^2$ erg s$^{-1}$. While

the other parameters of the fit depend weakly on the unconstrained value of $L_{\rm stand}$, this means that we cannot in principle rule out that the flat branch extends down to quiescence. However, we note that for H1743–322 and Swift J1753.5–0127, the two sources more similar to MAXI J1348–630, there is clear evidence that the standard track is followed in the low-flux regime (Coriat et al. 2011; Plotkin et al. 2017; Williams et al. 2020 ). Moreover, we note that points with $L_{\rm X} \gtrsim 10^{37}(D/2.2\ {\rm kpc})^2$ erg s$^{-1}$ seem to be more consistent with the steeper correlation $\beta = 1.4$, which is also shown for illustrative purpose in Fig. 1.

## 4 DISCUSSION

We have presented a detailed view of the radio/X-ray correlation of MAXI J1348–630 during its 2019/2020 outburst. The source clearly belongs to the growing population of outlier BHs. We traced the evolution of MAXI J1348–630 down to very low luminosities and observed it as it rejoined the standard correlation. Spanning six orders of magnitude in X-ray luminosity, the observations collected on MAXI J1348–630 constitute the most complete data set of an outlier obtained over a single outburst.

### 4.1 Evidence for an hybrid correlation

We find that MAXI J1348–630 is a new member of a restricted group of sources which appear to transition between the two known tracks. This particular behaviour, labelled hybrid (Xie & Yuan 2016), has already been observed (usually only partially) in H1743–322 (Coriat et al. 2011; Williams et al. 2020), Swift J1753.5–0127 (Plotkin et al. 2017), XTE J1752–223 (Ratti et al. 2012), MAXI J1659–152 (Jonker et al. 2012), GRS 1739–278 (Xie, Yan & Wu 2020), MAXI J1535–571 (Russell et al. 2019a; Parikh et al. 2019), and MAXI J1631–472 (Monageng et al. 2021). However, MAXI J1348–630 is, after H1743–322, only the second source in this regime to have such detailed monitoring, allowing the radio/X-ray behaviour to be so well constrained. Other sources classified as outliers have not been observed at such low luminosity (e.g. Corbel et al. 2004; Brocksopp et al. 2005). In fact, all outliers could also belong to the hybrid class (Motta et al. 2018, see Bahramian et al. 2018 for a global display of the diagram). The path of MAXI J1348–630 in the radio/X-ray diagram agrees well with H1743–322 (Jonker et al. 2010; Coriat et al. 2011). We note that, while both sources display a steep correlation at high luminosities and re-join the standard track before approaching quiescence, MAXI J1348–630 overall spans a broader range in $L_{\rm R}$ and $L_{\rm X}$, and is significantly fainter in radio than H1743–322 in the flat part of the correlation. Moreover, the transition luminosity between the two correlations is harder to identify in MAXI J1348–630 than in H1743–322, for which Coriat et al. (2011) find $L_{\rm trans} \simeq 5 \times 10^{36}$ erg s$^{-1}$ assuming a distance of 8 kpc, corresponding to $\sim 5 \times 10^{-3} L_{\rm Edd}$, and for which the standard track is reached at $\sim 5 \times 10^{-5} L_{\rm Edd}$. This is higher than what is inferred for MAXI J1348–630 in this work. If we assume a 7 M$_\odot$ BH (Tominaga et al. 2020; Carotenuto et al. 2021), the indicative value of $L_{\rm trans} \simeq 7 \times 10^{35}(D/2.2\,{\rm kpc})^2$ erg s$^{-1}$ corresponds to a transition happening at $\sim 7 \times 10^{-4}(D/2.2\ {\rm kpc})^2 L_{\rm Edd}$, while MAXI J1348–630 would re-join the standard track at the low value of $\sim 10^{-6}(D/2.2\ {\rm kpc})^2 L_{\rm Edd}$. It is important to note that our monitoring was conducted during a single outburst (including the following reflares), while the data on H1743–322 were accumulated over multiple outbursts (Coriat et al. 2011; Williams et al. 2020).

### 4.2 The radio-quiet hypothesis

There is not yet a universal consensus on the origin of the two tracks and on what drives the change in correlation of a given source on the radio/X-ray diagram. As outlined by Coriat et al. (2011), the two groups might be characterized by different levels of radio emission, possibly arising from different jet properties. Standard track sources and outliers could be labelled as, respectively, radio-loud and radio-quiet. As suggested by Motta et al. (2018), the existence of two populations on the diagram may be the result of geometric effects, rather than intrinsic differences between sources. Low inclination sources could appear radio-louder due to geometry and Doppler boosting, and thus would lie on the standard track. While we still lack a precise estimation of the MAXI J1348–630 inclination angle $\theta$, considerations on the discrete ejecta proper motion yield $\theta \lesssim 45^\circ$ (Carotenuto et al. 2021). Hence, as a medium-low inclination source, geometric effects might not be suited to explain the fainter level of radio emission from MAXI J1348–630, similarly to what has been found for MAXI J1535–571 (Parikh et al. 2019; Russell et al. 2019a). However, misaligned jets are possible (e.g. Miller-Jones et al. 2019).

Alternatively, physical differences between compact jets from different systems might be at the basis of the observed dichotomy on the diagram. Hints of a radio spectral difference between standard sources and outliers have been found by Espinasse & Fender (2018), possibly supporting this hypothesis. Compact jets powered by MAXI J1348–630 showed an average spectral index $\langle\alpha\rangle = 0.14 \pm 0.01$, which is more in agreement with a standard-track source than with an outlier. We tested the agreement with a Kolmogorov–Smirnov test on our spectral index distribution against the Gaussian distributions from Espinasse & Fender (2018), similarly to Williams et al. (2020). The null hypothesis was our distribution being consistent either with the standard or with the outlier distribution. For the outlier case, we find a $p$-value of $\sim 10^{-5}$, while we obtain a $p$-value of 0.33 when we test our distribution against the standard one. Therefore, we are able to reject the null hypothesis in the first case, concluding that the jet spectral index distribution of MAXI J1348–630 is inconsistent with what is observed for the population of outliers. We cannot draw conclusions regarding the agreement with the distribution observed in standard sources.

If a physical difference in the jets can explain the two tracks, this could possibly imply a change in the properties or in the morphology of the jets when sources belonging to the hybrid correlation transition between the two groups, as argued in Koljonen & Russell (2019). This should produce observable effects, including, according to Espinasse & Fender (2018), a significant change in the radio spectral index distribution between the tracks. For MAXI J1348–630 we could not constrain the spectral index at low luminosities, hence we cannot confirm or rule out a potential radio spectral difference between the two tracks, but such effect is not observed in other sources (e.g. Shaposhnikov et al. 2007), questioning the validity of this scenario. Alternatively, outliers could be characterized by compact jets with higher magnetic fields with respect to standard track sources (Pe'er & Casella 2009). While we have no measurement on the jet's magnetic field in MAXI J1348–630, an evolution of the magnetic field throughout the outburst, possibly increasing with the accretion rate and, thus, with $L_{\rm X}$, could explain the observed hybrid correlation, as argued by Coriat et al. (2011).

### 4.3 The X-ray-loud hypothesis

An alternative approach is to invoke differences in the X-ray emission produced by the accretion flow between the two groups. It has been

proposed that sources on the outlier track could be characterized by radiatively efficient accretion flows (e.g. Coriat et al. 2011; Huang, Wu & Wang 2014), such as the Luminous Hot Accretion Flow (LHAF; Yuan & Zdziarski 2004), and would be brighter in X-rays than standard track sources. Those might in turn be modelled with the radiatively inefficient accretion flows, such as the Advection Dominated Accretion Flow (ADAF, e.g. Narayan & Yi 1994). Outliers could then be called X-ray-loud instead of radio-quiet. Switching between tracks, hybrid sources would change from an an inefficient ADAF in the low flux regime to an efficient LHAF at high luminosity (Coriat et al. 2011). This is also supported by the detection of hard X-ray cut-offs in the spectra of sources on the outlier track, implying an effective cooling of the electrons responsible for the Comptonization of disc photons (Koljonen & Russell 2019). It has been shown that the radiative efficiency of the accretion flow could depend on the mass accretion rate and hence on $L_{\rm X}$ (Narayan & Yi 1995), and a change from an ADAF to various types of LHAF is possible above a given critical luminosity $L_{\rm C} \propto 5\theta_{\rm e}^{3/2}\alpha_v^2\dot{M}_{\rm Edd}$, where $\theta_{\rm e} = k_{\rm b}T_{\rm e}/m_{\rm e}c^2$ is the electron temperature in keV and $\alpha_v$ is the viscosity parameter of the accretion disc (Xie & Yuan 2012). This would produce the outlier track. In the context of the accretion-jet model (Xie & Yuan 2016), different values of $\alpha_v$ lead to different $L_{\rm C}$, playing a key role in differentiating between standard track sources and outliers. The path of MAXI J1348–630 agrees quite well with this scenario, since it is consistent with the standard track at $L_{\rm X} \lesssim 10^{33}(D/2.2\ {\rm kpc})^2$ erg s$^{-1}$ and then moves to the flat part at the transition between the two tracks above $\sim 10^{33}(D/2.2\,{\rm kpc})^2$ erg s$^{-1}$, which could be a proxy for a low value of $L_{\rm C}$, and possibly a low $\alpha_v$. Future insights on the values of $\alpha_v$ (see for instance Tetarenko et al. 2018) and $\theta_{\rm e}$ (e.g. Koljonen & Russell 2019) would be crucial to quantify this agreement. A radiatively efficient accretion flow could also explain the behaviour of neutron star systems (NS XRBs), which are found to be generally fainter in radio than BH XRBs (e.g. Migliari & Fender 2006; Tudor et al. 2017). At a given $L_{\rm R}$, the observed $L_{\rm X}$ might be increased by the additional X-ray emission coming from the solid surface. However, given the various nature of NS systems (Tudor et al. 2017; Gallo et al. 2018), the global situation appears to be more complex and a full comparison with NS XRBs is beyond the scope of this Letter.

As an alternative, Meyer-Hofmeister & Meyer (2014) suggested the presence of a weak, cool inner accretion disc, which would bring the source to the steep track by providing additional soft photons for Comptonization in the corona. The inner disc, resulting from partial re-condensation of the coronal material, would be present in the hard state at $L_{\rm X} \gtrsim 10^{-4}L_{\rm Edd}$. Despite the difficulty of detecting such disc with the current X-ray instruments, this scenario appears to reproduce well the path on the diagram followed by H1743–322 (Meyer-Hofmeister & Meyer 2014). However, MAXI J1348–630 leaves the standard track at $\sim 10^{-6}(D/2.2\ {\rm kpc})^2 L_{\rm Edd}$, and the existence of such disc is unlikely at these low accretion rates.

While there is yet no consensus on what produces the observed tracks, it will be crucial for future monitorings of hybrid correlation sources to obtain a deep and dense coverage of the outburst, especially close to the transition luminosities and in the low-flux regime. Constraining the radio/X-ray correlation at low luminosities will allow us to discriminate between the existing models and to improve our understanding of the disc/jet connection among X-ray binaries.

## ACKNOWLEDGEMENTS

We thank the anonymous referee for the careful reading of the manuscript and for providing valuable comments. We thank the staff at the South African Radio Astronomy Observatory (SARAO) for scheduling these observations. The MeerKAT telescope is operated by the SARAO, which is a facility of the National Research Foundation, an agency of the Department of Science and Innovation. This work was carried out in part using facilities and data processing pipelines developed at the Inter-University Institute for Data Intensive Astronomy (IDIA). IDIA is a partnership of the Universities of Cape Town, of the Western Cape and of Pretoria. FC, SC, and TDR thank Jamie Stevens and staff from the Australia Telescope National Facility (ATNF) for scheduling the ATCA radio observations. ATCA is part of the ATNF which is funded by the Australian Government for operation as a National Facility managed by CSIRO. We acknowledge the Gomeroi people as the traditional owners of the ATCA observatory site. We thank *Swift* for scheduling the X-ray observations. We acknowledge the use of data obtained from the High Energy Astrophysics Science Archive Research Center (HEASARC), provided by NASA's Goddard Space Flight Center. This research has made use of MAXI data provided by RIKEN, JAXA, and the MAXI team. FC acknowledges support from the project Initiative d'Excellence (IdEx) of Université de Paris (ANR-18-IDEX-0001). TDR acknowledges financial contribution from the agreement ASI-INAF no. 2017-14-H.0. We thank P. Saikia and W. Yu for their useful comments. We acknowledge the use of the Nançay Data Center, hosted by the Nançay Radio Observatory (Observatoire de Paris-PSL, CNRS, Université d'Orléans), and supported by Region Centre-Val de Loire.

## DATA AVAILABILITY

The un-calibrated MeerKAT and ATCA visibility data are publicly available at the SARAO and ATNF archives, respectively, at https://archive.sarao.ac.za and https://atoa.atnf.csiro.au. The *Swift*/XRT data are instead available from the *Swift* archive: https://www.swift.ac.uk/swift_portal, while the MAXI data can be downloaded from http://maxi.riken.jp/mxondem.

## REFERENCES

Al Yazeedi A., Russell D. M., Lewis F., Baglio M. C., Bramich D. M., Saikia P., 2019, Astron. Telegram, 13188, 1
Bahramian A. et al., 2018,Radio/X-Ray Correlation Database for X-ray Binaries , https://doi.org/10.5281/zenodo.1252036
Belloni T. M., Motta S. E., 2016, Transient Black Hole Binaries. Springer-Verlag, Berlin, p. 61
Bright J. et al., 2020, Nat. Astron., 4, 1
Brocksopp C., Corbel S., Fender R. P., Rupen M., Sault R., Tingay S. J., Hannikainen D., O'Brien K., 2005, MNRAS, 356, 125
Burrows D. N. et al., 2005, Space Sci. Rev., 120, 165
Camilo F. et al., 2018, ApJ, 856, 180
Carotenuto F. et al., 2020, Astron. Telegram, 14029, 1
Carotenuto F. et al., 2021, MNRAS, 504, 444
Chauhan J. et al., 2021, MNRAS, 501, L60
Corbel S. et al., 2000, A&A, 359, 251
Corbel S., Nowak M. A., Fender R. P., Tzioumis A. K., Markoff S., 2003, A&A, 400, 1007

Corbel S., Fender R. P., Tomsick J. A., Tzioumis A. K., Tingay S., 2004, ApJ, 617, 1272
Corbel S. et al., 2013, MNRAS, 428, 2500
Coriat M. et al., 2011, MNRAS, 414, 677
Corral-Santana J. M., Casares J., Muñoz-Darias T., Bauer F. E., Martínez-Pais I. G., Russell D. M., 2016, A&A, 587, A61
Dinçer T. et al., 2014, ApJ, 795, 74
Espinasse M., Fender R., 2018, MNRAS, 473, 4122
Falcke H., Körding E., Markoff S., 2004, A&A, 414, 895
Fender R. et al., 2018, Proc. of MeerKAT Science: On the Pathway to the SKA, 13
Gallo E., Fender R. P., Pooley G. G., 2003, MNRAS, 344, 60
Gehrels N. et al., 2004, ApJ, 611, 1005
Gallo E. et al., 2014, MNRAS, 445, 290
Gallo E., Degenaar N., van den Eijnden J., 2018, MNRAS, 478, L132
Gallo E. et al., 2019, MNRAS, 488, 191
Hannikainen D. C. et al., 1998, A&A, 337, 460
Huang C.-Y., Wu Q., Wang D.-X., 2014, MNRAS, 440, 965
Jonas J., MeerKAT Team, 2016, in Proc. of MeerKAT Science: On the Pathway to the SKA, 13
Jonker P. G. et al., 2010, MNRAS, 401, 1255
Jonker P. G. et al., 2012, MNRAS, 423, 3308
Koljonen K. I. I., Russell D. M., 2019, ApJ, 871, 26
Lamer G., Schwope A. D., Predehl P., Traulsen I., Wilms J., Freyberg M., 2021, A&A, 647, A7
Matsuoka M. et al., 2009, PASJ, 61, 999
Merloni A., Heinz S., di Matteo T., 2003, MNRAS, 345, 1057
Meyer-Hofmeister E., Meyer F., 2014, A&A, 562, A142
Migliari S., Fender R. P., 2006, MNRAS, 366, 79
Miller-Jones J. C. A. et al., 2019, Nature, 569, 374
Monageng I. M., Motta S. E., Fender R., Yu W., Woudt P. A., Tremou E., Miller-Jones J. C. A., van der Horst A. J., 2021, MNRAS, 501, 5776
Motta S. E., Casella P., Fender R. P., 2018, MNRAS, 478, 5159
Narayan R., Yi I., 1994, ApJ, 428, L13
Narayan R., Yi I., 1995, ApJ, 452, 710
Negoro H. et al., 2020, Astron. Telegram, 13994, 1
Parikh A. S. et al., 2019, ApJ, 878, L28
Pe'er A., Casella P., 2009, ApJ, 699, 1919
Pirbhoy S. F., Baglio M. C., Russell D. M., Bramich D. M., Saikia P., Yazeedi A. A., Lewis F., 2020, Astron. Telegram, 13451, 1
Plotkin R. M., Markoff S., Kelly B. C., Körding E., Anderson S. F., 2012, MNRAS, 419, 267
Plotkin R. M. et al., 2017, ApJ, 848, 92
Ratti E. M. et al., 2012, MNRAS, 423, 2656
Remillard R. A., McClintock J. E., 2006, ARA&A, 44, 49
Russell T. D. et al., 2019a, ApJ, 883, 198
Russell D. M., Al Yazeedi A., Bramich D. M., Baglio M. C., Lewis F., 2019b, Astron. Telegram, 12829, 1
Shaposhnikov N., Swank J., Shrader C. R., Rupen M., Beckmann V., Markwardt C. B., Smith D. A., 2007, ApJ, 655, 434
Shaw A. W. et al., 2021, ApJ, 907, 34
Tetarenko B. E., Sivakoff G. R., Heinke C. O., Gladstone J. C., 2016, ApJS, 222, 15
Tetarenko B. et al., 2018, Nature, 554, 69
Tominaga M. et al., 2020, ApJ, 899, L20
Tremou E. et al., 2020, MNRAS, 493, L132
Tudor V. et al., 2017, MNRAS, 470, 324
Williams D. R. A. et al., 2020, MNRAS, 491, L29
Xie F.-G., Yuan F., 2012, MNRAS, 427, 1580
Xie F.-G., Yuan F., 2016, MNRAS, 456, 4377
Xie F.-G., Yan Z., Wu Z., 2020, ApJ, 891, 31
Yatabe F. et al., 2019, Astron. Telegram, 12425, 1
Yuan F., Zdziarski A. A., 2004, MNRAS, 354, 953
Zhang L. et al., 2020, MNRAS, 499, 851

## SUPPORTING INFORMATION

Supplementary data are available at *MNRASL* online.

**Table S1**. Radio flux densities and unabsorbed X-ray fluxes selected for the radio/X-ray correlation presented in this work, along with the radio spectral index (when available) and the telescopes used for obtaining the data (see Carotenuto et al. 2021).

**Figure S1**. Hardness intensity diagram (HID) of MAXI J1348–630 during its main outburst, where the hardness ratio (HR) was determined from MAXI data.

Please note: Oxford University Press is not responsible for the content or functionality of any supporting materials supplied by the authors. Any queries (other than missing material) should be directed to the corresponding author for the article.

This paper has been typeset from a TEX/LATEX file prepared by the author.